Paclitaxel Combined with Inhibitors of Glucose and Hydroperoxide Metabolism Enhances Breast Cancer Cell Killing *Via* H$_2$O$_2$-Mediated Oxidative Stress

Tanja Hadzic, **Nükhet Aykin-Burns**, **Yueming Zhu**, **Mitchell C. Coleman**, **Katie Leick**, **Geraldine M. Jacobson**, and **Douglas R. Spitz**[*]
Free Radical and Radiation Biology Program, Department of Radiation Oncology, Holden Comprehensive Cancer Center, The University of Iowa, Iowa City, IA

Abstract

Cancer cells (relative to normal cells) demonstrate alterations in oxidative metabolism characterized by increased steady-state levels of reactive oxygen species [*i.e.* hydrogen peroxide, H$_2$O$_2$] that may be compensated for by increased glucose metabolism but the therapeutic significance of these observations is unknown. In the current study, inhibitors of glucose [*i.e.,* 2-deoxy-D-glucose, 2DG] and hydroperoxide [*i.e.,* L-buthionine-S, R-sulfoximine, BSO] metabolism were utilized in combination with a chemotherapeutic agent paclitaxel [PTX], thought to induce oxidative stress, to treat breast cancer cells. 2DG+PTX were found to be more toxic than either agent alone in T47D and MDA-MB231 human breast cancer cells, but not in normal human fibroblasts or normal human mammary epithelial cells. Increases in parameters indicative of oxidative stress, including steady-state levels of H$_2$O$_2$, total glutathione, and glutathione disulfide accompanied the enhanced toxicity of 2DG+PTX in cancer cells. Antioxidants, including N-acetyl-cysteine [NAC], polyethylene glycol-conjugated catalase [PEG-CAT] and superoxide dismutase [PEG-SOD], inhibited the toxicity of 2DG+PTX and suppressed parameters indicative of oxidative stress in cancer cells, while inhibition of glutathione synthesis using BSO further sensitized breast cancer cells to 2DG+PTX. These results show that combining inhibitors of glucose [2DG] and hydroperoxide [BSO] metabolism with PTX selectively (relative to normal cells) enhances breast cancer cell killing *via* H$_2$O$_2$-induced metabolic oxidative stress, and suggests that this biochemical rationale may be effectively utilized to treat breast cancers.

Keywords

breast cancer; hydroperoxide metabolism; metabolic oxidative stress; 2-deoxy-D-glucose; chemo-sensitization; cancer vs. normal cells

Introduction

PTX, also known as taxol, is an effective chemotherapeutic agent that is used widely for the treatment and management of breast carcinomas. PTX is routinely combined with

anthracycline-based chemotherapy regimens to treat high-risk breast cancers but is also effective as a single agent [1,2]. The mechanism by which PTX affects malignant cell division is thought to include hyperstabilization of microtubules and inhibition of cytoskeletal restructuring. These processes are thought to be essential during cell division [3,4]. The inability of PTX to hyperstabilize microtubules has been associated with development of resistance to this drug [5]. It has also been suggested that PTX can increase hydroperoxide production causing oxidative stress [6], but the relationship of oxidative stress to the overall mechanism by which PTX kills cancer cells is not well understood.

Glucose metabolism has been suggested to be an integral component of the intracellular metabolic hydroperoxide detoxification pathways, and glucose deprivation-induced cytotoxicity in breast cancer cells is believed to be, at least in part, mediated by metabolic oxidative stress [7–9]. It has been hypothesized that cancer cells compensate for defects in oxidative metabolism by increasing glucose metabolism to help detoxify hydroperoxides *via* pyruvate and NADPH dependent reactions [7–8]. Since cancer cells demonstrate increased utilization of glucose, as well as increased steady-state levels of hydroperoxides [7–8], we hypothesized that inhibitors of glucose and hydroperoxide metabolism would enhance the susceptibility of cancer cells to chemotherapeutic agents [*i.e.* PTX] thought to act *via* metabolic oxidative stress.

2DG is a glucose analog that is able to competitively inhibit glucose uptake and metabolism [9]. Since PTX and 2DG have both been suggested to kill cancer cells *via* oxidative stress, the current experiments were designed to determine if treatment of human breast carcinoma cells with 2DG could enhance the cytotoxicity of PTX *via* increases in metabolic oxidative stress, as well as demonstrate the involvement of reactive oxygen species (ROS; H_2O_2 and $O_2^{\bullet-}$) in the observed effects.

The results of the current studies show that treatment of both T47D and MDA-MB231 human breast cancer cells with the combination of 2DG and PTX leads to increases in parameters indicative of oxidative stress [*i.e.* H_2O_2 and GSSG] and enhanced cancer cell killing. An inhibitor of glutathione synthesis, BSO, further sensitized human breast cancer cells to the toxicity of 2DG+PTX. Furthermore, the non-specific thiol antioxidant [NAC], as well as specific scavengers of H_2O_2 and $O_2^{\bullet-}$ [catalase and superoxide dismutase, respectively], inhibited the increased cell killing seen with 2DG+PTX. These findings strongly support the hypothesis that the combination of 2DG and PTX leads to increased cytotoxicity *via* enhanced metabolic oxidative stress. These results also support the hypothesis that combined modality cancer therapies designed to inhibit glucose and hydroperoxide metabolism, while increasing pro-oxidant production with commonly used chemotherapeutic agents, may provide a useful biochemical rationale for the treatment of breast cancer.

Experimental Procedures

Cell Culture and Treatments

MDA-MB231 and T47D human breast cancer cells were obtained from the American Type Culture Collection [Manassas, VA] and maintained in RPMI 1640 media supplemented with 10% fetal bovine serum [FBS; Hyclone, Logan, UT]. Normal (non-immortalized) human mammary epithelial cells (HMEC) were purchased from Clonetics (East Rutherford, NJ) and maintained in MEBM media (Clonetics). GM00038 normal skin fibroblasts were obtained from the Coriell Institute [Camden, NJ] and maintained in Eagle's Minimum Essential Medium with Earle's salts supplemented with 10 % FBS, L-glutamine, vitamins, essential and non-essential amino acids. Cell cultures were maintained in 5% CO_2 and air in a humidified 37 ° C incubator in the presence of antibiotics [0.1% gentamycin]. 2-Deoxy-D-glucose [2DG], N-acetyl-cysteine [NAC], L-buthionine-[S, R]-sulfoximine, diphenyleneiodium [DPI] and

apocynin [APO] were obtained from Sigma [St. Louis, MO]. Paclitaxel [PTX] was purchased from Mayne Pharma Incorporated [Mulgrave, Australia]. Drugs were added to cells at the final concentrations of 20 mM 2DG, 20 mM NAC, 10 μM DPI, 10 μM APO, 1 mM BSO, and 0.1 μM PTX. Stock solutions of 1 M NAC [in 1 M sodium bicarbonate pH 7.4] were added directly to the cell cultures to obtain the desired concentration. Stock solutions of 1 mM APO and 1 mM DPI were dissolved in dimethylformamide and dimethyl sulfoxide, respectively, with the final concentration of 0.1% in media (vehicle alone controls were also included). Stock solutions of 1 mM PTX, 0.1 M BSO and 1 M 2DG, were dissolved in PBS and the required volume was added directly to the cells to achieve the desired final concentrations. The fluorescent dyes, oxidation sensitive MitoSOX [2 μM] and 5- [and-6]-carboxy-2′, 7′-dichlorodihydrofluorescein diacetate [CDCFH$_2$; 10 μg/ml], as well as the oxidation insensitive 5- [and-6]-carboxy-2′, 7′-dichlorofluorescein diacetate [CDCF; 10 μg/ml] and Mito\Tracker green [100 nM], were purchased from Molecular Probes [Eugene, OR], dissolved in DMSO, and added at a final concentration of 0.1% DMSO. Polyethylene glycol [PEG], polyethylene glycol catalase [PEG-CAT], and polyethylene glycol superoxide dismutase [PEG-SOD] were purchased from Sigma [St. Louis, MO] and added at the final concentration of 100 U/ml. PEG alone at the same concentration (18 μM) was added as the control.

Pro-oxidant Production

Pro-oxidant production was determined using the oxidation-sensitive 5- [and-6]-carboxy-2′, 7′-dichlorodihydrofluorescein diacetate [CDCFH$_2$; 10 μg/ml] and the oxidation insensitive 5- [and-6]-carboxy-2′, 7′-dichlorofluorescein diacetate [CDCF; 10 μg/ml] fluorescent probes [dissolved in DMSO] as described previously [9].

Clonogenic Cell Survival

Attached and floating cells in the experimental dishes were collected after trypsinization with 1x trypsin-EDTA [CellGro, Herndon, VA], centrifuged, re-suspended in fresh media, and counted using a Coulter Counter. Cells were then plated at low density and clones were allowed to grow for 14 days in complete media in the presence of 0.1% gentamycin. Cells were then fixed with 70% ethanol and stained with Coomassie Blue dye for analysis of clonogenic cell survival as previously described [10].

Glutathione Assay

Cell pellets collected from human breast cancer cells after various treatments were pipette-homogenized in 50 mM PO$_4$ buffer pH 7.8 containing 1.34 mM diethylenetriaminepentaacetic acid [DETAPAC buffer]. Total glutathione content was determined using the Anderson method [11]. To distinguish reduced glutathione [GSH] and glutathione disulfide [GSSG], 2 μl of a 1:1 mixture of 2-vinylpyridine and ethanol was added per 30 μl of sample and assayed as described previously [12]. All glutathione determinations were normalized to the protein content of whole homogenates using the method of Lowry *et al.* [13].

HPLC NAC Measurements

Cell pellets were thawed and homogenized in DETAPAC buffer, while the protein was determined using the method of Lowry *et al.* [13]. First, the thiols in the 20 μl of samples were derivatized by adding 230 μl Nanopure water [Barnstead-Thermolyne Corp., Dubuque, IA] and then 750 μl of 0.5 mM 9-Acetoxy-2-[4-[2,5-dihydro-2,5-dioxo-1H-pyrrol-1-yl]phenyl]-3-oxo-3H-naphtho{2,1-b}pyran [ThioGlo-3; dissolved in acetonitrile; Covalent Technologies, Inc., Walnut Creek, CA]. After 5 minutes at 37°C, the samples were acidified by adding a 1:6 dilution of 12 N HCl, in order to achieve a pH of 2.5. Samples were then filtered through 0.45 μm nylon syringe filters and separated on a Shimadzu high-pressure liquid chromatography [HPLC] system. The isocratic solvent system that was used as a mobile phase included 65%

acetonitrile, 35% water with 0.05% glacial acetic acid and 0.05% of 85% O-phosphoric acid with a flow rate of 0.5 ml/min and a fluorescent detector with excitation/emission wavelengths of 365 and 445 nm, respectively. Shimadzu Class VP software was used to obtain and analyze the data. NAC levels were normalized to the protein content of whole-cell homogenates.

Confocal Microscopy

Localization of superoxide production in cells was visualized using confocal microscopy. MDA-MB231 cells [200,000 cells] were plated on microscope slides and after 6 hours, treated with 20 mM 2DG and 0.1 μM PTX. After 24-hours, monolayer cultures were washed with PBS and then labeled with MitoSOX red (Molecular Probes) [2 μM; 0.11% DMSO] and MitoTracker green [100 nM; 0.11% DMSO] for 20 min in PBS [containing 5 mM pyruvate] at 37°C. Cells were analyzed using Zeiss LSM 510 confocal laser-scanning system [excitation 488 nm and 543 nm]. Images were acquired with a 63 X 1.4 NA Apochromat objective [Zeiss]. For quantification of fluorescence intensities, non-saturated images were taken with a full-open pinhole. During multi-channel imaging, each fluorescent dye was imaged sequentially in the frame-interlace mode to eliminate cross-talk between the channels. Images were acquired using 4 slices at the depth of 0.5 μm and all image processing was performed using the Zeiss LSM 5 Image Examiner software with identical background and gain settings. Six to eight areas were randomly picked and the representative images were collected.

Statistics

Statistical analysis was performed using GraphPad Prism version 4.0 for Windows [GraphPad Software, San Diego, CA]. To determine differences between three or more means, one-way or two-way ANOVA test was done with Tukey's post-hoc analysis. Error bars represent standard error of the mean [SEM] unless otherwise specified. P-values <0.05 were accepted as statistically significant.

Results

The final concentration of 20 mM 2DG was chosen for cell culture experiments to ensure maximal competitive inhibition of glucose metabolism in RPMI culture medium containing 11 mM glucose and 0.1 μM PTX was chosen as a clinically relevant drug dose that can be easily achieved in humans [1,2,9]. When MDA-MB231 and T47D cells were assayed for cell growth in the presence of 20 mM 2DG, 0.1 μM PTX or 2DG+PTX for 0–48 hours, cells treated with 2DG+PTX experienced the largest growth inhibition relative to the control cells [data not shown]. These differences in growth were most significant at 48 hrs time when comparing the untreated cells to 2DG-, PTX- and 2DG+PTX-treated cells [data not shown]. Due to the fact that more cells remained attached to the culture dishes at 24 hours, relative to 48 hours, the 24 hour time point was selected for subsequent experiments when examining the mechanisms responsible for drug-induced cytotoxicity.

Treatment of exponentially growing MDA-MB231 and T47D cells with 20 mM 2DG or 0.1 μM PTX for 24 hours caused a significant decrease in cell survival (20–25% and 60–70%, respectively) compared to the control cells, but the combination of 2DG+PTX resulted in the greatest increase in clonogenic cell killing [90–95% of MDA-MB231 and T47D] when compared to either agent alone [Fig 1A]. These results support the conclusion that the toxicity of 2DG+PTX is at least additive in these human breast cancer cell lines [Fig 1A].

To determine if oxidative stress mediated by H_2O_2 was contributing to 2DG+PTX-induced cytotoxicity, steady-state levels of H_2O_2 were assayed by measuring catalase [a specific H_2O_2 scavenger] inhibitable oxidation of 5- [and-6]-carboxy-2′, 7′-dichlorodihydrofluorescein diacetate [CDCFH$_2$]. When MDA-MB231 and T47D cells were exposed to 0.1 μM PTX or

2DG+PTX for 24 hours in the absence [Fig 1B] and presence [Fig 1C] of 100 U/ml PEG-CAT significant 3- and 5-fold increases [relative to the control cells] in PEG-CAT inhibitable probe oxidation [indicative of increases in steady-state H_2O_2] were observed [Fig 1D]. In the control and 2DG groups approximately 33–50% of the signal is inhibitable by PEG-CAT indicating that in these treatment groups 33–50% of the MFI is mediated by H_2O_2, depending on the cell line. In the PTX and 2DG+PTX groups 67–80% of the signal is inhibitable by PEG-CAT indicating that in these treatment groups 67–80% of the signal is mediated by H_2O_2. Most importantly, in the presence of PEG-CAT none of the treatment groups differ from their respective control strongly supporting the conclusion that all the drug induced differences between the treatment groups were mediated by H_2O_2. Interestingly, steady-state levels of probe oxidation both in the presence and absence of PEG-CAT detected with this assay were significantly higher in T47D cells than in MDA-MB231 cells [Fig 1B–D]. Since T47D cells also consumed significantly higher levels of glucose than MDA-MB231 cells [data not shown], these results may suggest that intracellular steady-state levels of H_2O_2 could be greater in cells with a greater requirement for glucose metabolism, but a rigorous analysis of this relationship goes beyond the scope of the current experiments.

To ensure that changes in CDCFH$_2$ fluorescence measured in Figure 1B–D were detecting changes in probe oxidation, and not changes in cell size, probe uptake, ester cleavage of the probe, and probe efflux [independent of changes in probe oxidation] the previous experiments were repeated using the oxidation insensitive analog of CDCFH$_2$ [CDCF]. The data in Figure 1E show no differences among treatment groups when the cells were labeled with CDCF, which supports that conclusion that changes fluorescence that were being detected in Figures 1B–D were caused by changes in the oxidation of CDCFH$_2$. Overall, the results in Figure 1B–E strongly support the conclusion that treatment of cells with PTX or PTX+2DG caused significant increases in steady-state levels of intracellular H_2O_2 in both human breast cancer cell lines.

In order to determine the role of ROS (i.e., H_2O_2 and $O_2^{\bullet-}$) in cell killing induced by 2DG +PTX, MDA-MB231 and T47D cells were treated with 20 mM 2DG + 0.1 μM PTX for 24 hours in the presence and absence of 100 U/mL PEG-CAT and/or PEG-SOD [a specific $O_2^{\bullet-}$ scavenger]. PEG-CAT was found to modestly inhibit 2DG- or PTX-induced clonogenic killing [data not shown]. In addition, PEG-CAT significantly inhibited the toxicity of 2DG +PTX in both MDA-MB231 and T47D cells [Fig 2A]. However, PEG-CAT appeared to protect the T47D breast cancer cells more effectively than the MDA-MB231 cells [Fig 2A]. PEG-SOD alone only modestly protected cells from 2DG+PTX but the combination of PEG-CAT+PEG-SOD completely protected both MDA-MB231 and T47D from clonogenic cell killing induced by 2DG+PTX [Fig 2A] during the 24 hour treatment interval. In contrast, PEG alone [not conjugated to the enzymes] did not protect cells from 2DG+PTX [Fig 2A]. Finally, when PEG-CAT was boiled to inactivate the enzyme, it no longer protected cells from 2DG and/or PTX toxicity [data not shown] indicating that enzymatic activity of catalase was required to produce the effect. These results support the conclusion that H_2O_2 and $O_2^{\bullet-}$ are responsible for the enhanced cytotoxicity seen when early exponential growth phase human breast cancer cells are treated with 2DG+PTX.

Previous studies using MCF-7 and HL-60 cells have suggested that the source of ROS production during PTX exposure might be the membrane bound NADPH oxidase enzyme [15]. To determine the contribution of NADPH oxidase enzymes to ROS production in our model system, MDA-MB231 human breast cancer cells were treated with NADPH oxidase inhibitors, 10 μM APO [A] or 10 μM DPI [B] for 24 hours, in the presence of 2DG and/or PTX [21–23]. The results in Supplemental Figure 1 demonstrate that neither APO [10 μM] nor DPI [10 μM] protected cells from clonogenic cell killing mediated by PTX or 2DG+PTX. These

results support the conclusion that in our model system NADPH oxidase enzymes did not contribute to the cytotoxicity of PTX or 2DG+PTX.

To determine whether mitochondria contributed to ROS production during exposure to 2DG +PTX, confocal microscopy was used to visualize mitochondria using MitoTracker green (100 nM), and the $O_2^{\bullet-}$ production was visualized by measuring MitoSOX red [Fig 2B] in MDA-MB231 cells. In Figure 2B [a] the red signal shows that, although the oxidation of MitoSOX occurred in every treatment group, prominent probe oxidation was observed in cells treated with PTX or 2DG+PTX. Furthermore the MitoTracker green signal [Fig 2B(b)] co-localized very well with the MitoSOX red oxidation signal [Fig 2B(c)] producing yellow signal. These results support the hypothesis that intracellular $O_2^{\bullet-}$ production in cells treated with 2DG and/ or PTX originated from mitochondria [Fig 2B].

To determine if disruptions in glutathione metabolism were involved in the oxidative stress and toxicity caused by 2DG+PTX, levels of total glutathione [GSH] and glutathione disulfide [GSSG] were measured in MDA-MB231 and T47D cell homogenates. When MDA-MB231 and T47D cells were treated for 24 hours with 20 mM 2DG or 0.1 μM PTX, 1.5- to 2.0-fold increases in total GSH content, were noted [Fig 3A]. Treatment of MDA-MB231 and T47D cells with the combination of 2DG+PTX resulted in 2.3- to 3.4-fold increases, respectively, in the levels of total GSH [Fig 3A]. Interestingly, in T47D breast cancer cells, the basal levels of total GSH that were significantly higher relative to MDA-MB231 [Fig 3A] consistent with the increased steady-state levels of H_2O_2 detected in these cells [Fig 1B]. Most importantly, MDA-MB231 cells treated with 2DG, PTX, or 2DG+PTX showed 3-fold, 5-fold, and 7-fold increases in GSSG, respectively, compared to the untreated cells [Fig 3B]. Since glutathione represents the major small molecular weight soluble thiol in cells, these results showed that 2DG or PTX are capable of inducing oxidative stress, as evidenced by increases in GSSG, and cells attempted to compensate for this by increasing the synthesis of GSH. Furthermore, the combination of 2DG+PTX appeared to enhance the severity of oxidative stress as well as cytotoxicity in MDA-MB231 breast cancer cells (Figures 3B and 1A). Interestingly, GSSG levels were below detection limits in T47D cells [data not shown]. To determine if undetectable GSSG levels in T47D cells could be attributed to altered glutathione reductase [GR] activity, GR levels were compared in both cell lines using the method described by Mavis and Stellwagen [14] and found to be three times higher in T47D cells than in MDA-MB231 cells [data not shown].

To determine if glutathione metabolism significantly contributed to 2DG+PTX-induced cytotoxicity, MDA-MB231 and T47D cells were treated with 1 mM BSO [an inhibitor of GSH synthesis] 1 hr before and during exposure to 10 mM 2DG and 0.05 μM PTX [Fig 4A]. BSO significantly enhanced clonogenic cell killing in the presence of 2DG+PTX [Fig 4A] as well as depleted total GSH at least 70% and inhibited drug-induced increases in total GSH [Fig 4B]. Interestingly, depletion of total GSH in MDA-MB231 cells with BSO resulted in the remaining fraction of total glutathione being nearly all in the disulfide form (Figure 4C). Also combining BSO with 2DG+PTX also enhanced endpoints indicative of oxidative stress in MDA-MB231 cells, as evidenced by significant increases in %GSSG [Fig 4C]. These results support the conclusion that compromising the metabolism of glutathione with an inhibitor of glutathione synthesis significantly enhances the toxicity of 2DG+PTX by a mechanism involving oxidative stress.

To determine if a non-specific thiol antioxidant, NAC, could protect human breast cancer cells from 2DG+PTX-induced toxicity, MDA-MB231 and T47D cells were treated with 20 mM NAC, 20 mM 2DG, 0.1 μM PTX and/or 1 mM BSO for 24 hours. Figures 5A and 5B show that NAC was able to enter the cells in the reduced form and protect them from 2DG+PTX-induced toxicity. Most importantly, NAC was also able to inhibit 2DG+PTX+BSO-mediated

toxicity and suppress increases in %GSSG without reversing the effects of BSO on GSH depletion [Fig 5C–D]. These results indicate that NAC inhibits metabolic oxidative stress associated with 2DG+PTX+BSO independent of increasing GSH levels, supporting the hypothesis that NAC is augmenting intracellular thiol antioxidant pools and inhibiting thiol oxidation reactions that do not depend entirely on the metabolism of GSH. These findings continue to support the conclusion that metabolic oxidative stress plays a causal role in 2DG +PTX+BSO-mediated breast cancer cell killing.

In order to determine if normal cells were sensitized to PTX-induced cell killing by 2DG, normal human skin fibroblasts [GM00038] and normal human mammary epithelial cells [HMECs] were treated with 20 mM 2DG and/or 0.1 μM PTX for 24 hours. Supplemental Figure 2 demonstrates that at the doses tested, using the same protocol as was used for the cancer cells, neither 2DG nor PTX [in the presence or absence of 2DG] caused clonogenic cell killing in the GM00038 normal human fibroblasts cells. Surprisingly, 2DG significantly enhanced the percentage of cells capable of forming colonies in the presence and absence of PTX, relative to the vehicle controls (Supplemental Figure 2). When the experiment was repeated with HMECs treated with 20 mM 2DG and/or 0.1 μM PTX for 24 hours in the presence and absence of 1 mM BSO, treatment with 2DG alone caused no significant clonogenic cell killing and PTX caused 40–50% clonogenic cell killing in these normal human mammary epithelial cells (Figure 6A). In contrast to what was seen in human breast cancer cells (Figure 1A), HMECs did not demonstrate additive toxicity when treated with 2DG+PTX (Figure 6A). Most importantly, when HMECs were treated with 2DG+PTX+BSO no significant cell killing was noted and 2DG+BSO appeared to protect HMECs from PTX-induced clonogenic cell killing [Fig 6A]. Overall, the findings in supplemental Figure 2 and Figure 6A clearly support the hypothesis that the 2 normal human cell types (GM00038 fibroblasts and HMECs) are far less susceptible to clonogenic cell killing mediated by the interaction of 2DG+PTX in the presence and absence of BSO when compared to the 2 human breast carcinoma cell lines (Figure 1 and 4).

Discussion

Although the mechanism by which PTX kills cancer cells is thought to involve the hyperstabilization of microtubules and inhibition of cytoskeletal restructuring associated with mitosis, metabolic oxidative stress has also been suggested to play a role in the antitumor effects of PTX [1–3]. It has been proposed by other authors that PTX can increase production of hydroperoxides and cause oxidative stress in human lung cancer cells and breast cancer cells [6,15]. Furthermore, in a report by Alexandre *et al*. a significant induction of H_2O_2 release at 1 hour of PTX treatment was noted in A549 lung cancer cells [15]. Also consistent with this hypothesis, treatment of human lung and breast cancer cells with PTX was shown to cause increases in endpoints indicative of oxidative stress [6,15]. Furthermore, the thiol antioxidants, NAC and reduced GSH, have been found by other authors to protect human lung cancer cells from the toxicity of PTX, and catalase was found to protect bystander cells from the toxicity of PTX [6,15]. These results all support the hypothesis that PTX may mediate its cytotoxic effects in cancer cells *via* the production of ROS such as hydrogen peroxide. However a definitive data demonstrating the relative involvement of H_2O_2 and $O_2^{•-}$ in the toxicity of PTX as well as data showing that inhibitors of glucose and hydroperoxide metabolism can enhance the toxicity of PTX *via* H_2O_2-induced oxidative stress are lacking.

It has been suggested that cancer cells demonstrate increased steady-state levels of hydroperoxides, relative to normal cells, because of defects in oxidative metabolism [8,16–19]. Cancer cells have been hypothesized to increase glucose metabolism in order to detoxify hydroperoxides *via* direct deacetylation reactions with α-keto acids [such as pyruvate formed during glycolysis], as well as through regeneration of NADPH [from the pentose cycle] which

acts as a co-factor for the glutathione and thioredoxin dependent peroxidase systems [8, Fig 6B]. The increased dependency of cancer cells on glucose and hydroperoxide metabolism for detoxification of hydroperoxides could represent a potential target when attempting to selectively sensitize cancer cells to therapeutic agents that induce oxidative stress. From this model [Fig 6B] we predicted that treating human breast cancer cells with inhibitors of glucose and hydroperoxide metabolism [2DG and BSO] in combination with a chemotherapeutic agent [PTX] that induces oxidative stress would significantly enhance breast cancer cell killing.

In order to determine if inhibition of glucose metabolism sensitized human breast cancer cells to the cytotoxicity and oxidative stress induced by exposure to PTX, MDA-MB231 and T47D clonogenic survival was measured after treatment of early, exponentially growing cultures with 20 mM 2DG and/or 0.1 μM PTX for 24 hours. It was observed that treatment of both breast cancer cell lines with 2DG and PTX alone decreased clonogenic cell survival but the combination of 2DG+PTX resulted in at least additive toxicity [Fig 1A]. Furthermore, increased steady-state levels of H_2O_2 were detected in both breast cancer cell lines treated with PTX and 2DG+PTX suggesting that metabolic oxidative stress mediated by H_2O_2 could be contributing to the cytotoxicity of this drug combination [1B-D]. When the cells were exposed to 2DG+PTX in the presence and absence of PEG-CAT [specific scavenger of H_2O_2] and PEG-SOD [specific scavenger of $O_2^{\bullet-}$] the results showed that PEG-CAT provided the most protection from 2DG+PTX-induced toxicity relative to PEG-SOD [Fig 2]. In addition, the protection that was observed was due to catalase enzymatic activity and not the PEG, showing that H_2O_2 was significantly contributing to the cytotoxicity of 2DG+PTX [Fig 2]. Interestingly, the combination of PEG-CAT+PEG-SOD was more effective at protecting MDA-MB231 cells than either enzyme alone, strongly suggesting that both H_2O_2 and $O_2^{\bullet-}$ were contributing to 2DG+PTX toxicity, as has been previously suggested for 2DG treatment in human head and neck cancer cells [20] as well as glucose deprivation in human prostate cancer cells [19].

To determine the origin of H_2O_2 and $O_2^{\bullet-}$ responsible for the toxicity of 2DG+PTX, NADPH oxidase inhibitors were utilized and found to offer no protection from clonogenic cell killing in our model system, suggesting that NADPH oxidase activity was not contributing to cell killing induced during exposure to 2DG+PTX (Supplemental Figure 1). In the next series of experiments the involvement of mitochondria in the ROS production seen during treatment with 2DG+PTX was visualized using confocal microscopy to monitor the site of MitoSOX red oxidation as a marker for intracellular $O_2^{\bullet-}$ production in combination with MitoTracker green as a marker for mitochondrial localization [Figure 2B]. Oxidation of the MitoSOX probe was most prominent in the PTX- and 2DG+PTX-treated cells and co-localized with MitoTracker green, indicating that these treatments cause an increase in intracellular $O_2^{\bullet-}$ production localized to mitochondria [Figure 2B]. These results support the hypothesis that mitochondria may be the major source of pro-oxidant [H_2O_2 and $O_2^{\bullet-}$] production during 2DG and/or PTX exposure. These findings are consistent with a report by Varbiro *et al.* [24], showing that PTX increased ROS production in isolated mitochondria. In this previous report, the authors propose that PTX-induced mitochondrial ROS production was greater in the lipid phase relative to the aqueous phase, suggesting that the ROS induced by PTX were localized mainly to the mitochondrial membrane [24].

To confirm that metabolic oxidative stress was involved in 2DG+PTX-induced toxicity, as well as to probe the involvement of cellular thiols in the response, total glutathione [GSH +GSSG] and glutathione disulfide [GSSG] were also measured. Total GSH and GSSG levels were found to be significantly increased in human breast cancer cells treated with 2DG+PTX [Fig 3A-B]. Since GSH is the most abundant soluble thiol in cells and functions as a cofactor for peroxide and electrophile detoxification through the activity of GPx and glutathione-S-transferase enzymes [25–27], increases in the levels of total GSH could represent an attempt by the 2DG+PTX-treated cells to enhance their peroxide [or electrophile] metabolic capability

in response to oxidative stress [8,19,25]. In addition, the fact that GSSG accumulates [a product of the GPx reaction with hydroperoxides] supports the hypothesis that GSH-dependent hydroperoxide metabolism may be compromised and the recycling of GSSG back to GSH *via* GR may be limited in cells treated with 2DG+PTX [28]. An equally viable alternative to this hypothesis which is also consistent with the current observations, is that 2DG+PTX enhances endoplasmic reticulum (ER) stress, resulting in ER calcium release, activation of mitochondrial ROS production, and tumor cell killing via oxidative stress [29–31]. Regardless of the exact pathway leading to H_2O_2-mediated oxidative stress, the results in the current report are all consistent with the hypothesis that 2DG+PTX treatment is inducing oxidative stress and thiol oxidation in human breast cancer cells that significantly contributes to clonogenic cell killing.

BSO is a relatively specific inhibitor of glutamate cysteine ligase [GCL; the rate-limiting enzyme in GSH synthesis; 27, 32] that has been tested in clinical trials as a chemosensitizing agent [32]. Based on our observation that GSH content was apparently increasing during treatment with 2DG+ PTX, it was reasoned that inhibition of GSH synthesis with BSO in combination with 2DG or PTX could further increase oxidative stress and cytotoxicity in human breast cancer cells. In support of this hypothesis, treatment with 2DG+PTX+BSO was found to inhibit the synthesis of GSH, enhance toxicity, and cause a significant increase in the %GSSG in human breast cancer cells, relative to cells treated with 2DG+PTX [Fig 4]. Interestingly, BSO alone also caused a significant increase in the %GSSG in breast cancer cells and this is thought to be due to the inability of cancer cells to effectively recycle GSSG to GSH in the presence of BSO due to relatively high steady-state levels of metabolic production of ROS [28]. Because 2DG and BSO are well-tolerated and relatively non-toxic agents [32–35], combining them with a chemotherapeutic agent [PTX] that increases steady-state levels of H_2O_2 could represent an effective means of selectively targeting breast cancer cells for killing *via* a mechanism involving metabolic oxidative stress, while allowing for a reduction in the systemic dose of the chemotherapeutic agent being used.

In order to establish that oxidative stress was causally related to the enhanced cell killing seen in the presence of BSO, cells were treated with 2DG+PTX+BSO in the presence of a non-specific thiol antioxidant, NAC. The results in Figure 5 showed that NAC inhibited cell killing as well as suppressed endpoints indicative of oxidative stress in breast cancer cells treated with 2DG+PTX+BSO [Fig 5]. Furthermore, it is clear that NAC suppressed the oxidative stress and cytotoxicity caused by 2DG+PTX+BSO by inhibiting thiol oxidation reactions that are independent of GSH synthesis, since GSH levels were nearly undetectable in 2DG+PTX+NAC +BSO treated cells [Fig 5]. Overall, these results strongly support the conclusion that the cytotoxicity and H_2O_2-mediated oxidative stress caused by 2DG+PTX in human breast cancer cells can be significantly enhanced by inhibition of GSH synthesis *via* a mechanism that appears to involve oxidative stress as well as thiol oxidation.

In conclusion, the current study supports the hypothetical relationships between cancer cell cytotoxicity, glucose metabolism, prooxidant production, chemotherapeutic agents, and cellular antioxidants that are illustrated in Fig 6B. Inhibition of breast cancer cell glucose metabolism could enhance cytotoxicity and oxidative stress by limiting the recycling of $NADP^+$ to NADPH *via* the pentose phosphate pathway or by decreasing the formation of pyruvate by glycolysis [19,28,36–40]. In addition, it is also possible that 2DG+PTX could enhance ER stress, resulting in ER calcium release, activation of mitochondrial ROS production, increased oxidative stress, and increased cytotoxicity [29–31]. Regardless of the pathway leading to H_2O_2-induced oxidative stress the results presented in this report are consistent with the biochemical rationale that inhibitors of glucose and hydroperoxide metabolism can be combined with chemotherapeutic agents that increase H_2O_2 and $O_2^{\bullet-}$

formation to provide an effective means for sensitization of malignant cells to metabolic oxidative stress [Fig 6B;9,20,28].

Our study is also the first to report the differential susceptibility of human breast cancer cells vs. normal human cells to clonogenic cell killing induced by 2DG+PTX in the presence and absence of BSO [Supplemental Figure 2 and Figure 6A]. This point is critically important since the efficacy of combined modality cancer therapies is in large part based upon the ability of cytotoxic agents to selectively kill cancer vs. normal cells. If relatively non-toxic (to normal cells) agents such as 2DG and BSO could selectively enhance oxidative stress in cancer cells, then they could be combined with toxic agents (such as PTX) that induce oxidative stress to selectively sensitize cancer vs. normal cells to oxidative stress induced cell killing while causing less normal tissue injury. The current data set together with previous data showing that breast cancer cells have significantly higher steady-state levels of H_2O_2 and $O_2^{\bullet-}$ that contributes to differential sensitivity of cancer vs. normal cells to 2DG-induced cell killing [28], continues to support the hypothesis that the differential susceptibility of cancer cells to 2DG+PTX could be due to fundamental differences in oxidative metabolism that exist between cancer vs. normal cells [8, 28]. Considering that PTX is already used widely in the treatment of human cancers, our findings may provide a novel biochemical rationale for the development of new combined modality therapies to enhance the therapeutic efficacy of PTX in the treatment of breast cancer.

Supplementary Material

Refer to Web version on PubMed Central for supplementary material.

Acknowledgments

Abbreviations

H_2O_2	Hydrogen peroxide
2DG	2-deoxy-D-glucose
BSO	L-buthionine-S, R-sulfoximine
PTX	paclitaxel
NAC	N-acetyl-cysteine
PEG-CAT	polyethylene glycol-conjugated catalase
PEG-SOD	polyethylene glycol-conjugated superoxide dismutase
$CDCFH_2$	5- [and-6]-carboxy-2′, 7′-dichlorodihydrofluorescein diacetate
CDCF	5- [and-6]-carboxy-2′, 7′-dichlorofluorescein diacetate
GSH	reduced glutathione
GSSG	glutathione disulfide

References

1. Holmes FA, Walters RS, Theriault RL, Forman AD, Newton H, Yasuda H, Karin M, Kikugawa K. Phase II trial of taxol, active drug in the treatment of metastatic breast cancer. J Natl Cancer Inst 1991;83:1797–1805. [PubMed: 1683908]

2. Liebmann J, Cook JA, Fisher J, Teague D, Mitchell JB. *In vitro* studies of taxol as a radiation sensitizer in human tumor cells. J Natl Cancer Inst 1994;86:441–446. [PubMed: 7907149]

3. Glass-Marmor L, Beitner R. Taxol [paclitaxel] induces a detachment of phosphofructokinase from cytoskeleton of melanoma cells and decreases the levels of glucose-1,6-biphosphate, fructose-1,6-biphosphate and ATP. Eur J Pharmacol 1999;370:195–199. [PubMed: 10323269]

4. Singh SP, Gao Y, Singh LD, Kunapuli SP, Revindra R. Role of microtubules in glucose uptake by C6 glioma cells. Pharmacol Toxicol 1998;83:83–89. [PubMed: 9783325]

5. Orr GA, Verdier-Pinard P, McDaid H, Horwitz SB. Mechanisms of taxol resistance related to microtubules. Oncogene 2003;22:7280–7295. [PubMed: 14576838]

6. Alexandre J, Batteux F, Nicco C, Chereau C, Laurent A, Guillevin L, Weill B, Goldwasser F. Accumulation of hydrogen peroxide is an early and crucial step for paclitaxel-induced cancer cell death both *in vitro* and *in vivo*. Int J Cancer 2006;119:41–48. [PubMed: 16450384]

7. Swatrowski TP, Nathan CF. Production of large amounts of hydrogen peroxide by human tumor cells. Cancer Res 1991;51:794–798. [PubMed: 1846317]

8. Spitz DR, Sim JE, Ridnour LA, Galoforo SS, Lee YJ. Glucose deprivation- Induced oxidative stress in human tumor cells: a fundamental defect in metabolism? Ann N Y Acad Sci 2000;899:349–362. [PubMed: 10863552]

9. Andringa KK, Coleman MC, Aykin-Burns N, Hitchler MJ, Walsh SA, Domann FE, Spitz DR. Inhibition of glutamate cysteine ligase activity sensitizes human breast cancer cells to the toxicity of 2-deoxy-D-glucose. Cancer Res 2006;66:1605–1610. [PubMed: 16452219]

10. Spitz DR, Malcolm R, Roberts R. Cytotoxicity and metabolism of 2- hydroxy-2-nonenol and 2-nonenol in H_2O_2-resistant cell lines. Do aldehydic by- products of lipid peroxidation contribute to oxidative stress? Biochem J 1990;267:453–459. [PubMed: 2334404]

11. Anderson, ME. Handbook of methods for oxygen radical research. Greenwald, RA., editor. Florida: CRC Press, Inc; 1985. p. 317-323.

12. Griffith OW. Determination of glutathione and glutathione disulfide using glutathione reductase and 2-vinylpyridine. Anal Biochem 1980;106:207–212. [PubMed: 7416462]

13. Lowry OH, Rosebrough NJ, Farr AL, Randall RL. Protein Measurements with the folin phenol reagent. J Biol Chem 1951;193:265–275. [PubMed: 14907713]

14. Mavis RD, Stellwagen E. Purification and subunit structure of glutathione reductase from bakers' yeast. J Biol Chem 1968;243:809–814. [PubMed: 5638597]

15. Alexandre J, Hu Y, Lu W, Pelicano H, Huang P. Novel action of paclitaxel against cancer cells: bystander effect mediated by reactive oxygen species. Cancer Res 2007;67:3512–3517. [PubMed: 17440056]

16. Blackburn RV, Spitz DR, Liu S, Galoforo SS, Sim JE, Ridnour LA, Chen JC, Davis BH, Corry PM, Lee YL. Metabolic oxidative stress activates signal transduction and gene expression during glucose deprivation in human tumor cells. Free Radic Biol Med 1990;26:419–430. [PubMed: 9895234]

17. Averill-Bates DA, Przybytkowski E. The role of glucose in cellular defenses against cytotoxicity of hydrogen peroxide in CHO cells. Arch Biochem Biophys 1994;312:52–58. [PubMed: 8031146]

18. Lin X, Zhang F, Bradbury CM, Kaushal A, Li L, Spitz DR, Aft RL, Gius D. 2-Deoxy-D-glucose-induced cytotoxicity and radiosensitization in tumor cells are mediated *via* disruptions in thiol metabolism. Cancer Res 2003;63:3413–3418. [PubMed: 12810678]

19. Ahmad IM, Aykin-Burns N, Sim JE, Walsh SA, Higashikubo R, Buettner GR, Venkataraman S, Mackey MA, Flanagan SW, Oberley LW, Spitz DR. Mitochondrial $O_2^{\bullet-}$ and H_2O_2 mediate glucose deprivation-induced cytotoxicity and oxidative stress in human cancer cells. J Biol Chem 2005;11:4254–4263. [PubMed: 15561720]

20. Simons AL, Ahmad IM, Mattson DM, Dornfeld KJ, Spitz DR. 2-Deoxy- D-glucose combined with cisplatin enhances cytotoxicity *via* metabolic oxidative stress in human head and neck cancer cells. Cancer Res 2007;67:3364–3370. [PubMed: 17409446]

21. Kassim T, Rajni S, Rajesh KT, Walter HW, Shyam B, Michael AT. Redox- regulation of Erk1/2-directed phosphatase by reactive oxygen species: Role in signaling TPA-induced growth arrest in ML-1 cells. J Cell Physiol 2008;216:276–285. [PubMed: 18270969]

22. Klees RF, De Marco PC, Salasznyk RM, Ahuja D, Hogg M, Antoniotti S, Kamath L, Dordick JS, Plopper GE. Apocynin derivatives interrupt intracellular signaling resulting in decreased migration in breast cancer cells. J Biomed Biotechnol 2006;2:87246–87250. [PubMed: 16883056]

23. Kallio A, Zheng A, Dahllund J, Heiskanen KM, Härkönen P. Role of mitochondria in tamoxifen-induced rapid death of MCF-7 breast cancer cells. Apoptosis 2005;10:1395–1410. [PubMed: 16215679]

24. Varbiro G, Veres B, Gallyas FJ, Sumegi B. Direct effect of taxol on free radical formation and mitochondrial permeability transition. Free Radic Biol Med 2001;31:548–558. [PubMed: 11498288]

25. Aft RL, Zhang FW, Gius D. Evaluation of 2-deoxy-D-glucose as a chemotherapeutic agent: mechanism of cell death. Br J Cancer 2002;87:805–812. [PubMed: 12232767]

26. Spitz DR, Kinter MT, Roberts RJ. The contribution of increased glutathione content to mechanisms of oxidative stress resistance in hydrogen peroxide resistant hamster fibroblasts. J Cell Physiol 1995;165:600–609. [PubMed: 7593239]

27. Arrick BA, Griffith OW, Cerami A. Inhibition of glutathione synthesis as a chemotherapeutic strategy for trypanosomiasis. J Exp Med 1981;153:720–725. [PubMed: 7252412]

28. Aykin-Burns N, Ahmad IM, Zhu Y, Oberley LW, Spitz DR. Increased levels of superoxide and hydrogen peroxide mediate the differential susceptibility of cancer cells versus normal cells to glucose deprivation. Biochem J 2009;418:29–37. [PubMed: 18937644]

29. Kurtoglu M, Gao N, Shang J, Maher JC, Lehrman MA, Wangpaichitr M, Savaraj N, Lane AN, Lampidis TJ. Under normoxia, 2-deoxy-D-glucose elicits cell death in select tumor types not by inhibition of glycolysis but by interfering with N-linked glycosylation. Mol Cancer Ther 2007;6:3049–58. [PubMed: 18025288]

30. Hung JY, Hsu YL, Ni WC, Tsai YM, Yang CJ, Kuo PL, Huang MS. Oxidative and endoplasmic reticulum stress signaling are involved in dehydrocostuslactone-mediated apoptosis in human non-small cell lung cancer cells. Lung Cancer. Epub ahead of print] Aug 21, 2009.

31. Lee WL, Wen TN, Shiau JY, Shyur LF. Differential proteomic profiling identifies novel molecular targets of paclitaxel and phytoagent deoxyelephantopin against mammary adenocarcinoma cells. J Proteome Res. Epub ahead of print Nov 25, 2009.

32. Bailey HH. L-S, R-buthionine sulfoximine: historical development and clinical issues. Chem Biol Interact 1998;111–112:239–254.

33. Landau BR, Lubs HA. Animal responses to 2-Deoxy-d-glucose administration. Procl Soc Exp Bio Med 1958;99:124–127.

34. Mohanti BK, Rath GK, Anantha N, Kannan V, Das BS, Chandramouli BA, Banerjee AK, Das S, Jena A, Ravichandran R, Sahi UP, Kumar R, Kapoor N, Kalia VK, Dwarakanath BS, Jain V. Improving cancer radiotherapy with 2-Deoxy-D-glucose: phase I/II clinical trials on human cerebral gliomas. Int J Radiat Oncol Biol Phys 1996;35:103–11. [PubMed: 8641905]

35. Maschek G, Savaraj N, Priebe W, Braunschweiger P, Hamilton K, Tidmarsh GF, De Young LR, Lampidis TJ. 2-Deoxy-D-glucose increases the efficacy of adriamycin and paclitaxel in human osteosarcoma and non-small cell lung cancers *in vivo*. Cancer Res 2004;64:31–34. [PubMed: 14729604]

36. Nath KA, Ngo EO, Heggel RP. Ketoacids scavenge H_2O_2 *in vitro* and *in vivo* and reduce menandione-induced DNA injury and cytotoxicity. Am J Physiol 1995;268:227–236.

37. Di Monaco M, Pizzini A, Gatto V, Leonardi L, Gallo M, Brignardello E, Boccuzzi G. Role of glucose-6-phosphate dehydrogenase inhibition in the antiproliferative effects of dehydroepiandrosterone on human breast cancer cells. Br J Cancer 1997;75:589–592. [PubMed: 9052415]

38. Berggren MI, Husbeck B, Samulitis B, Baker AF, Gallegos A, Powis G. Thioredoxin peroxidase-1 [peroxiredoxin-1] is increased in thioredoxin-1 transfected cells and results in enhanced protection against apoptosis caused by hydrogen peroxide but not by other agents including dexamethasone, etoposide, and doxorubicin. Arch Biochem Biophy 2001;392:103–109.

39. Nomura K, Imai H, Koumura T, Arai M, Nakagawa Y. Mitochondrial phospholipid hydroperoxide glutathione peroxidase suppresses apoptosis mediated by a mitochondrial death pathway. J Biol Chem 1999;274:29294–29302. [PubMed: 10506188]

40. Tuttle SW, Varnes ME, Mitchell JB, Biaglow JE. Sensitivity to chemical oxidants and radiation in CHO cell lines deficient in oxidative pentose cycle activity. Int J Radiat Oncol Biol Phys 1992;22:671–675. [PubMed: 1544835]
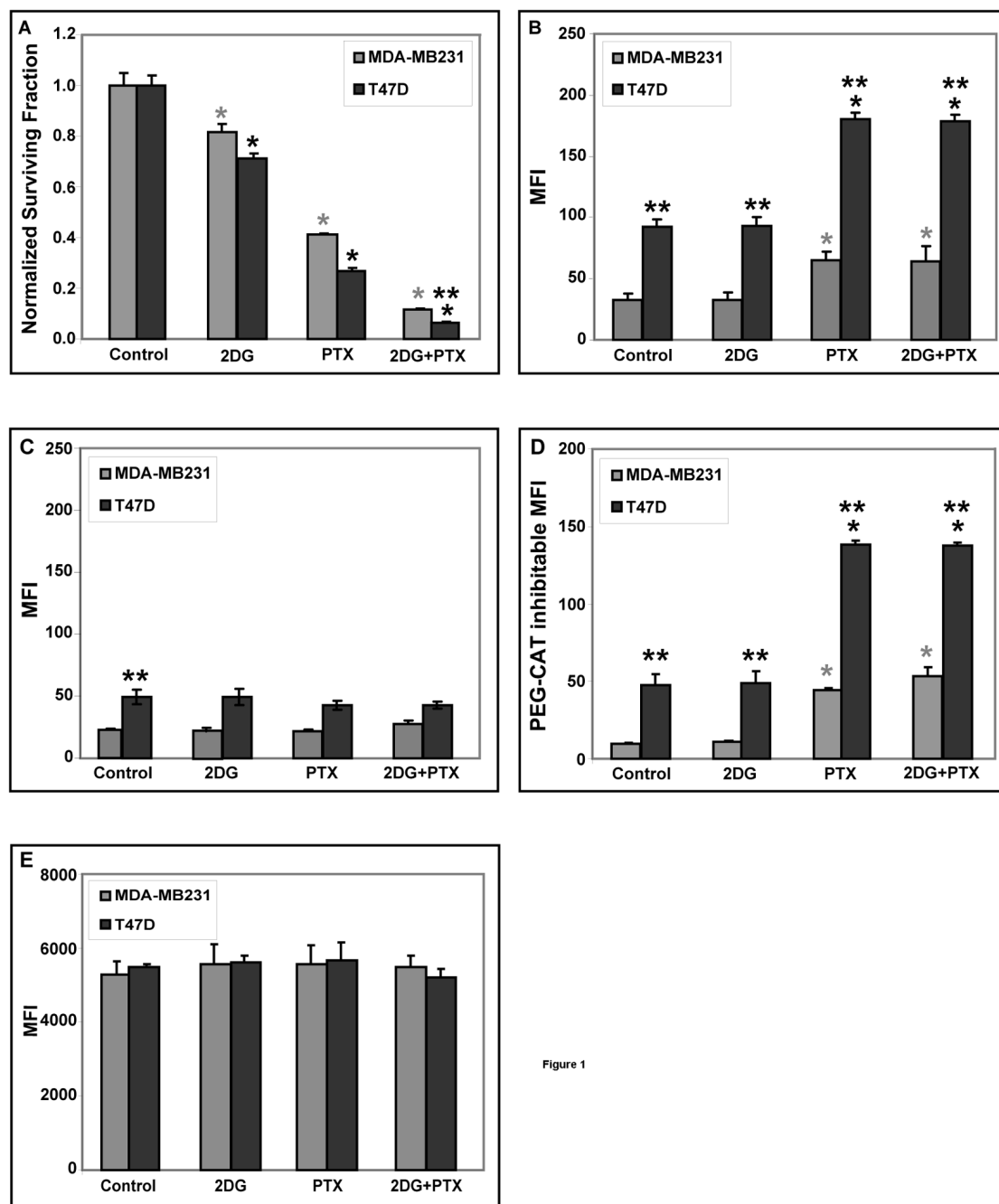
Figure 1. Treatment of MDA-MB231 and T47D cells with 2DG+PTX enhances clonogenic cell killing and increases pro-oxidant production
Cells were plated at 300,000–400,000 cells per 60-mm dish. [A] After 6 hours, cells were treated with 20 mM 2DG and/or 0.1 μM PTX and incubated for 24 hours. Cells were then collected for the clonogenic cell survival. The graphs represent the data from three independent experiments. [B-D] Steady-state levels of H_2O_2 were determined using the PEG-CAT inhibitable signal from the oxidation sensitive $CDCFH_2$ probe and flow cytometry analysis. Cells exposed to 20 mM 2DG and/or 0.1 μM PTX were either pre-treated [C] or not pre-treated [B] with 100 U/mL PEG-CAT for 2 hours before and again during the labeling period. After drug treatment, cells were trypsinized and harvested on ice, washed once and re-suspended in

PBS on ice. Cells in panel [B] were labeled with the oxidation sensitive [CDCFH$_2$] or in panel [E] with the oxidation insensitive [CDCF] fluorescent probe for 15 minutes at 37°C. PEG-CAT inhibitable mean florescence intensity (MFI) was calculated by subtracting the MFI values measured in the presence of PEG-CAT from that measured in the absence of PEG-CAT [panel D]. After labeling cells were placed on ice and analyzed by flow cytometry [excitation 488 nm, emission 585 nm]. The MFI of labeled cells was determined using 10,000 cells per sample and then corrected for autofluorescence from unlabeled cells. [n=3]. *: $P < 0.05$ versus the respective controls; **: $P < 0.05$ MDA-MB231 versus T47D cells.
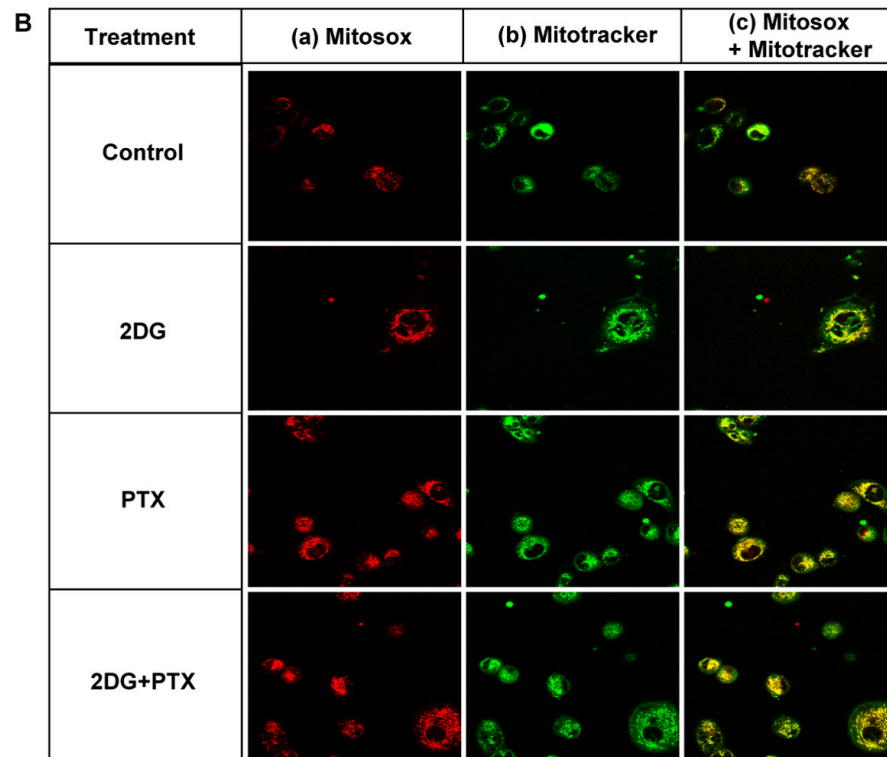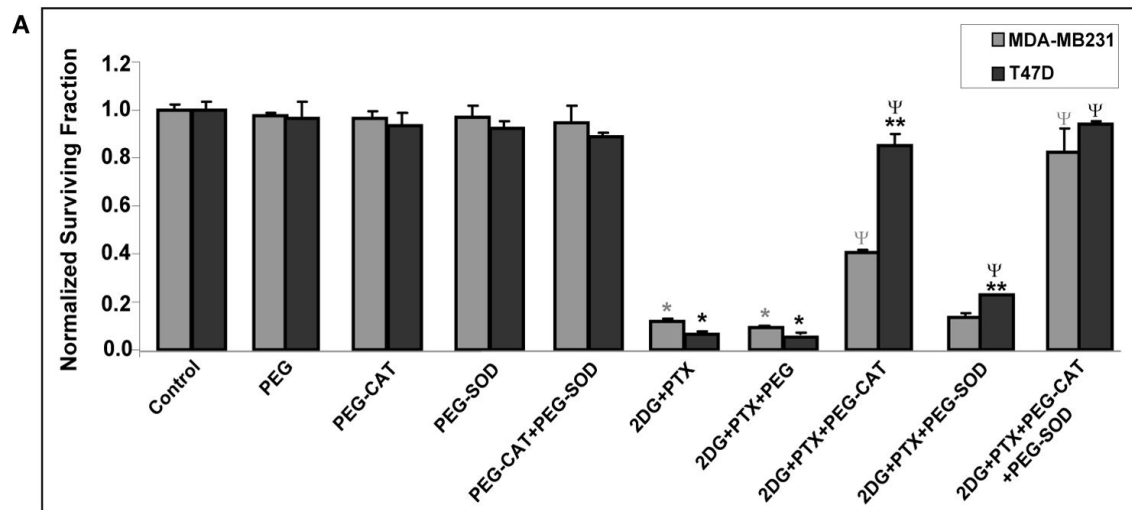
Figure 2. Treatment of MDA-MB231 and T47D cells with PEG-CAT+PEG-SOD protects from 2DG+PTX-mediated clonogenic cell killing

[A] Cells were plated and treated as in Figure 1. [A] Cells were treated in the presence and absence of 18 μM PEG alone, 100 U/ml PEG-CAT and/or 100 U/ml PEG-SOD. Cells were then harvested for the clonogenic cell survival assay. The graph represents the data from three independent experiments. [B] Cells were plated [100,000–200,000 cells/dish] and treated as in Figure 1. Cells were also labeled with MitoSOX [2 μM] and MitoTracker [100 nM] for 20 minutes at 37°C. Cells were then placed on ice and visualized using confocal microscopy. The figure shows representative data from two separate experiments performed in duplicate. Cells labeled red indicate MitoSOX oxidation; cells stained green indicate MitoTracker, and

superimposed images in yellow indicate co-localization of MitoSOX and MitoTracker. *: P < 0.05 versus the respective controls; **: P < 0.05 MDA-MB231 versus T47D cells; Ψ: P < 0.05 versus respective 2DG+PTX.
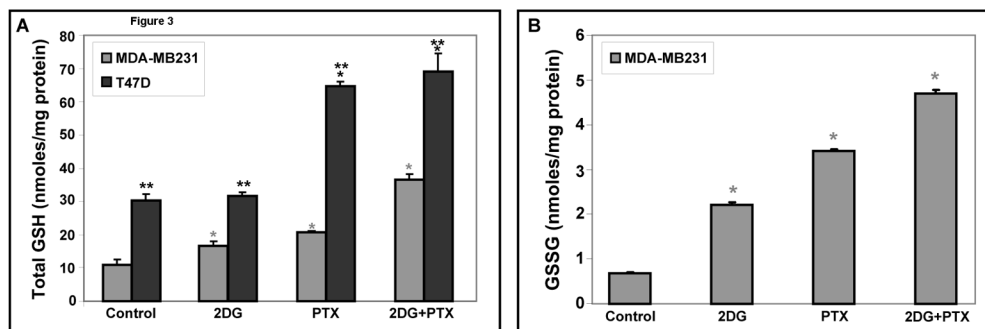
Figure 3. Total GSH and GSSG levels are significantly increased in human breast cancer cells treated with 2DG+PTX

MDA-MB231 and T47D breast cancer cells were plated [2,000,000–3,000,000 cells/100-mm dish] and allowed to recover from trypsinization for 6 hours. Cells were then treated with 20 mm 2DG and/or 0.1 μM PTX for 24 hours. After treatment, cells were scrape-harvested in cold PBS and the pellets allowed to freeze/thaw before the samples were homogenized and various assays were performed [n=3]. Results are presented in GSH equivalents per mg protein. Panels [A] and [B] represent the measurements of total GSH [GSH+GSSG] and GSSG, respectively.*: $P < 0.05$ versus the respective controls; **: $P < 0.05$ MDA-MB231 versus T47D cells.
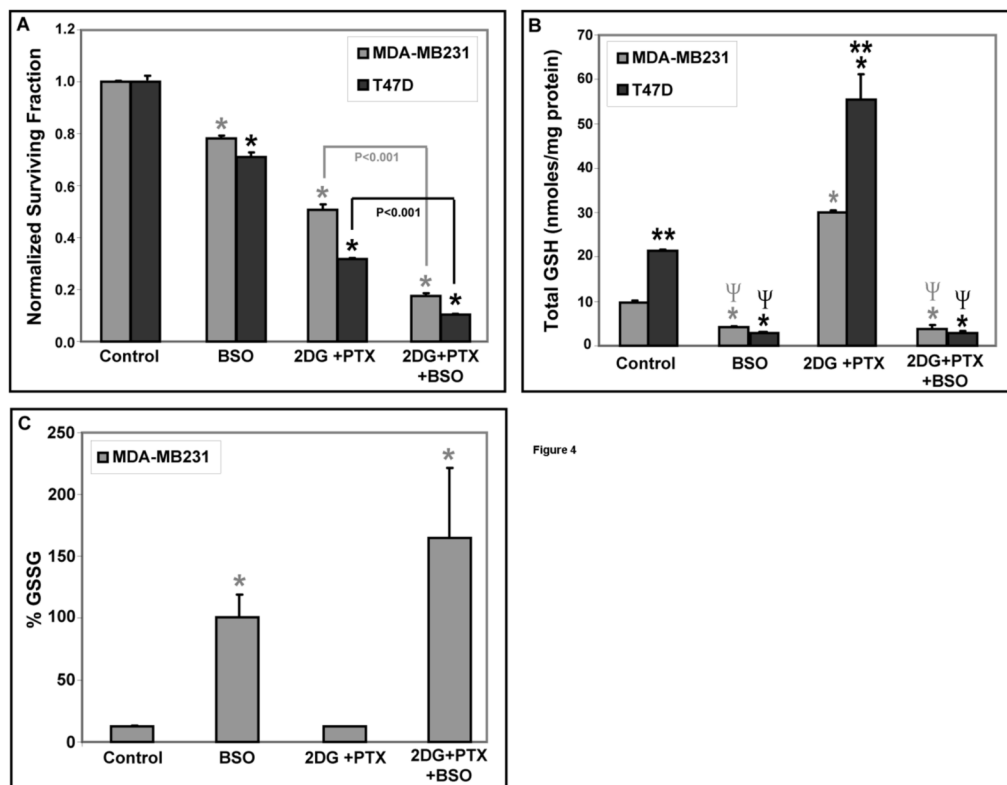
Figure 4. Oxidative stress and cytotoxicity induced by 2DG+PTX is significantly enhanced by depleting GSH with BSO

[A] Cells were plated at 300,000–400,000 cells per 60-mm dish and incubated for 6 hours. Cells were treated with 1 mM BSO 1 hour before and during 24-hour exposure to 10 mM 2DG and/or 0.05 μM PTX. After treatment, cells were assayed for cell surviving fraction using the clonogenic cell survival assay [n=3]. [B-C] MDA-MB231 and T47D breast cancer cells were plated [2,000,000–3,000,000 cells/100-mm dish] and allowed to recover from trypsinization for 6 hours. Cells were then treated with 20 mm 2DG and/or 0.1 μM PTX for 24 hours. After treatment, cells were scrape-harvested in cold PBS and cell pellets allowed to freeze/thaw before glutathione assay was performed [n=3]. Panels [B] and [C] represent the measurements of total GSH [GSH+GSSG] and GSSG, respectively in GSH equivalents. *: P < 0.05 versus the respective untreated control cells; **: P < 0.05 MDA-MB231 versus T47D cells; Ψ: P < 0.05 versus 2DG+PTX-treated cells.
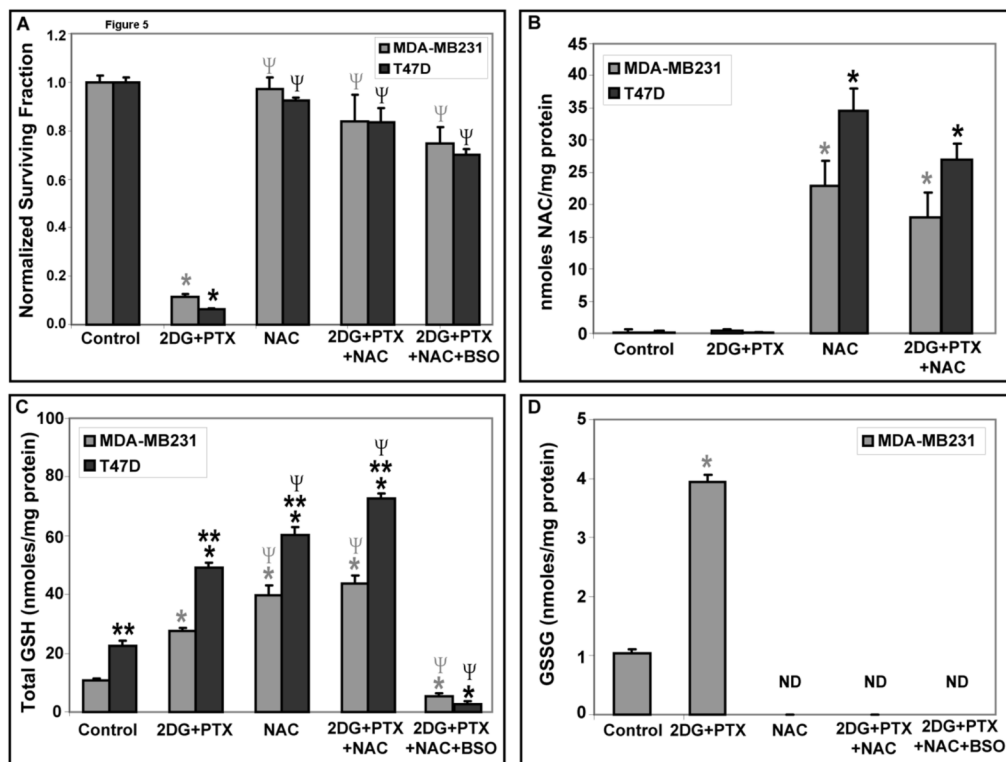
Figure 5. The thiol antioxidant, NAC, protect cells from clonogenic cell killing mediated by 2DG +PTX

[A] Cells were plated and treated as in Figure 4 with 20 mM 2DG, 0.1 μM PTX, 1 mM BSO or 20 mM NAC for 24 hours. After treatment, cells were assayed using the clonogenic cell survival assay [n=3]. [B-D] For thiol analysis, MDA-MB231 and T47D breast cancer cells were plated [2,000,000–3,000,000 cells/100-mm dish]. After 6–8 hours, cells were treated with 20 mm 2DG, 0.1 μM PTX, 1 mM BSO or 20 mM NAC for 24 hours. Following treatment, cells were scrape-harvested using cold PBS and cell pellets allowed to freeze/thaw before glutathione or HPLC assays were performed on homogenates [n=3]. Panel [B] represents measurement of intracellular NAC by HPLC; Panels [C] and [D] represent measurements of total GSH and GSSG, respectively. *: P < 0.05 versus the respective controls. **: P < 0.05 MDA-MB231 versus T47D; Ψ: P <0.05 versus the respective 2DG+PTX group; ND=not detectable.
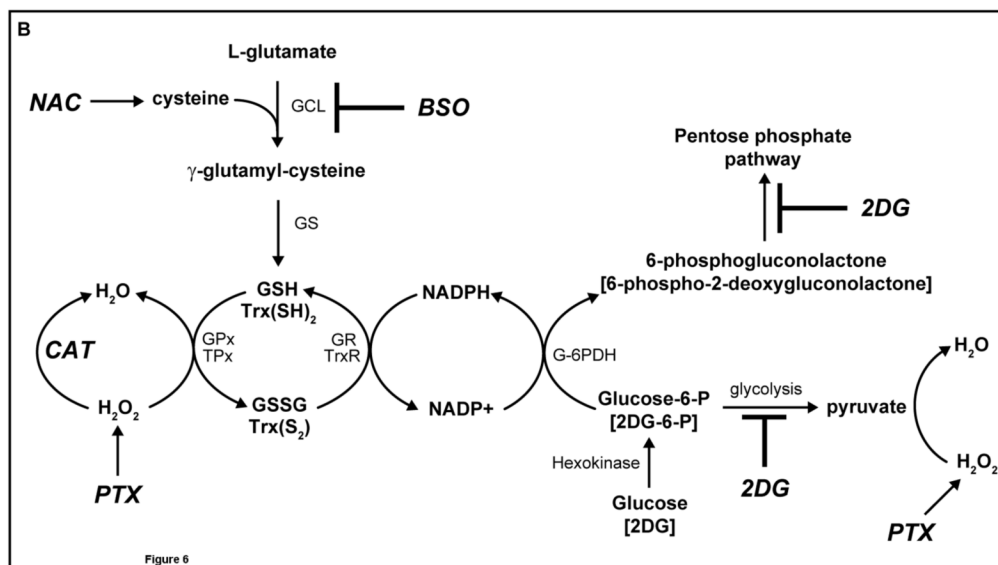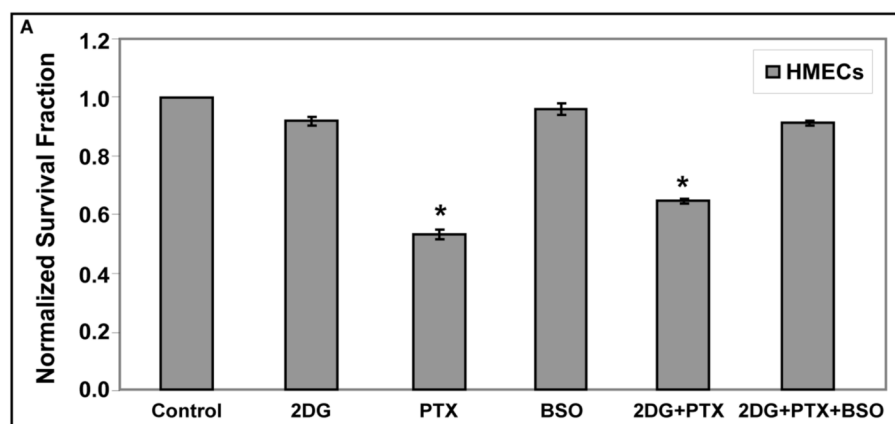
Figure 6. PTX- and/or 2DG-induced clonogenic cell killing in HMECs (panel A) and a theoretical model outlining potential mechanisms involved in the interaction between 2DG and PTX
[A] Cells were plated at 200,000 cells per 60-mm dish. After 6 hours, cells were treated with 20 mM 2DG, 0.1 μM PTX and/or 1 mM BSO and incubated for 24 hours. Cells were then collected and plated for the clonogenic cell survival. The graphs represent the data of 5–6 cloning dishes counted from each treatment dish done in three independent experiments. *: P < 0.05 versus the control. [B] 2DG competes with glucose for entry into cells and phosphorylation by hexokinase into 2-deoxy-D-glucose-6-phosphate [2DG-6-P] and glucose-6-phophate [G-6-P], respectively. G-6-P continues into the glycolytic pathway to generate pyruvate, a known scavenger of hydrogen peroxide [H_2O_2], while 2DG-6-P is unable to continue through glycolysis. G-6-P and 2DG-6-P can both proceed through the first step in the pentose phosphate pathway *via* G-6-P dehydrogenase [G-6-PDH] to 6-phosphogluconolactone and 6-phospho-2-deoxygluconolactone, respectively, leading to regeneration of NADPH from $NADPH^+$. However, 6-phospho-2-deoxygluconolactone cannot proceed further in the pentose phosphate pathway. NADPH serves as the source of reducing equivalents for the glutathione peroxidase/glutathione reductase [GPx/GR] and thioredoxin peroxidase/thioredoxin reductase [TPx/TR] systems. The glutathione [GSH] and thioredoxin [Trx] systems participate in the detoxification of H_2O_2 and other organic hydroperoxides. SOD dismutes superoxide [$O_2^{\bullet-}$] to H_2O_2 and CAT or GPx (TPx) convert H_2O_2 to H_2O. NAC supplies cysteine, which reacts with L-glutamate to form γ–glutamyl-cysteine *via* glutamate

cysteine ligase [GCL], which is inhibited by BSO. Glutathione synthetase [GS] converts γ–glutamyl-cysteine to GSH.